

Thermal-Chemical Instability in Plasma Assisted Ignition

Hongtao Zhong¹, Mikhail N. Shneider¹, Mikhail S. Mokrov², and Yiguang Ju¹

¹Department of Mechanical and Aerospace Engineering, Princeton University,
Princeton, NJ 08544, USA

²Institute for Problems in Mechanics, RAS, Moscow, Russia

E-mail: hongtaoz@princeton.edu

May 2019

Abstract. The control of plasma instability in plasma assisted ignition is of great importance to achieve efficient volumetric ignition for advanced lean burn engines. In this work, we proposed a new concept of plasma chemical instability and analyzed the mechanisms and impact of plasma chemical instability on the transition from a uniform discharge to a contracted state of a self-sustained glow discharge in a H₂-O₂-N₂ mixture. A one-dimensional numerical model for plasma chemical instability was developed which accounted for convective loss, Joule heating of plasma, and major non-equilibrium plasma assisted combustion kinetic pathways including electron-impact ionization, vibrational energy transfer, electron attachment, and combustion reactions and heat release. The results showed the plasma chemical instability significantly modified the onset plasma current of plasma thermal instability. Specifically, the critical current of the instability transition was strongly influenced by electron attachment to oxygen, fuel pyrolysis, electron-impact reactant ionization, endothermic/exothermic combustion reactions, and the formation of combustion products.

Submitted to: *J. Phys. D: Appl. Phys.*

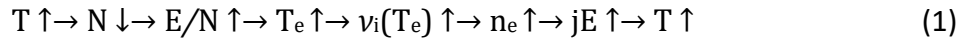
Keywords: Plasma Thermal Instability, Plasma Chemical Instability, Plasma-assisted Ignition, Hydrogen

1. Introduction

The call for carbon reduction and energy sustainability requires the development of ultra-lean combustion engine technology [1], which has a higher efficiency and lower carbon and pollutant emissions. Therefore, realization of reliable ignition for ultra-lean mixtures is critical to the development of advanced internal combustion (IC) engines [2] and gas turbines [3]. However, the traditional spark ignition systems are difficult to be applied to ignite ultra-lean fuel mixtures due to the small spark volume and the rapid increase of the critical ignition radius with the decrease of the mixture equivalence ratio [4, 5]. As such, there is a critical need to develop a novel concept to achieve volumetric ignition for engine operations at ultra-lean conditions.

Recent studies show that non-equilibrium plasma is a promising technique to facilitate ultra-lean combustion and improve engine performance via the increase of plasma discharge volume [6, 7, 8]. Specially, streamers in a combustible mixture are volumetric and their contraction into multiple thin channels will provide a promising technique to achieve volumetric ignition [9]. The transition from volumetric plasma discharge to thin hot channels is called plasma thermal-ionization instability or plasma thermal instability [10, 11].

Plasma thermal instability has been studied extensively in noble gases and air. The occurrence of plasma thermal instability is explained by the thermal-ionization mechanism [11]. For example, at isobaric conditions, a temperature perturbation from the local Joule heating induces thermal expansion and increases the reduced electric field (E/N). Consequently, the ionization process controlled by the reduced electric field is amplified exponentially to trigger higher production rate of electrons and more intense heating. The positive feedback of the thermal-ionization mechanism is expressed as,



Previous experimental studies [12] about plasma thermal instability were mostly conducted in a tube with diffusive cooling or in a weakly ionized gas flow. It was observed that the discharge contracted non-uniformly: the contracted channel was formed in the vicinity of one electrode, then gradually grew toward the other electrode. Shneider et al. developed two-dimensional modeling of the plasma thermal instability in nitrogen in a planar geometry [13] and in air in an axisymmetric cylindrical geometry [14]. The results showed that transition of the volumetric uniform plasma to the contracted state had a hysteresis cycle, which allowed the coexistence of both volumetric and contracted states. By applying a sufficient perturbation, the volumetric plasma could abruptly transform into an unstable or contracted state. However, most previous studies of plasma were limited to noble gases and air. How plasma instability would occur in combustible mixtures during the plasma assisted ignition processes is not well-understood.

In plasma assisted combustion [8], with plasma-generated energetic electrons and active radicals and excited species, the plasma enhanced fuel decomposition and oxidation in a combustible mixture will have strong kinetic effects on plasma instability via the changes of electron number density, electron energy, electric field, and plasma induced combustion heat release. Therefore, in addition to the classical plasma thermal instability, the plasma assisted combustion pathways may trigger a new plasma chemical instability (PCI) via a chemical kinetic mechanism. Unfortunately, to the authors' knowledge, few

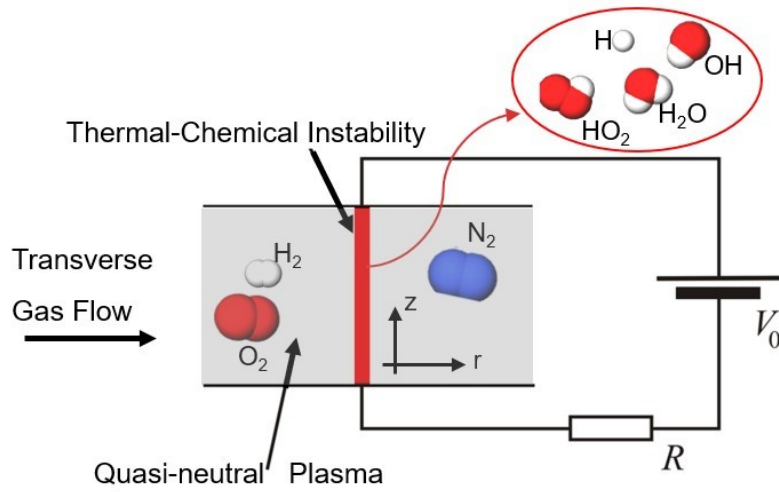


Figure 1: Schematic illustration of the computational model for the plasma chemical instability in $\text{H}_2\text{-O}_2\text{-N}_2$ mixtures. The geometry is axisymmetric cylindrical. Plasma enhanced combustion chemical kinetics will influence the plasma instability both thermally and kinetically.

studies have been attempted to understand the plasma instability affected by plasma chemistry.

The objective of this work is to present and validate a new concept of plasma chemical instability caused by plasma combustion chemistry. At first, a set of one-dimensional simplified self-consistent governing equations for plasma assisted ignition is formulated. Then, numerical simulations are conducted to understand the mechanisms and dynamics of plasma chemical instability of $\text{H}_2\text{-O}_2\text{-N}_2$ mixtures in the DC discharge gas flow. Several possible coupling mechanisms between plasma kinetics and combustion kinetics for plasma chemical instability will be identified. Finally, the effect of critical parameters for the onset of plasma chemical instability will be discussed.

2. One-dimensional Model for Spatial-Temporal Dynamics of Plasma Chemical Instability

Plasma thermal instability is intrinsically three-dimensional due to the presence of the plasma-induced flow motion. As this work focuses on the new concept of plasma chemical instability via the couplings between plasma and combustion chemical kinetics, we only analyze the instability in the initially homogeneous quasi-neutral axisymmetric positive column by using a simplified radial-dependent one-dimensional model [14] (shown in Fig. 1). The dynamics of near electrode sheath layers is neglected since their thickness is much smaller than the gap between the two electrodes. The role played by the sheath layers in the current analysis is limited to be a source of perturbations.

The governing equations relate the densities of electrons, n_e , positive ions, n_+ , and negative ions, n_- , electric field, E , translational gas temperature, T , and the vibrational temperature, T_v . The continuity equations for n_e , n_- , and n_+ are,

$$\frac{\partial n_e - O \cdot (\mu_e n_e E + D_e O n_e)}{\partial t} = Q_e \quad (2)$$

$$\frac{\partial n_- - O \cdot (\mu_- n_- E)}{\partial t} = Q_- \quad (3)$$

$$\frac{\partial n_+ + O \cdot (\mu_+ n_+ E)}{\partial t} = Q_+ = Q_e + Q_- \quad (4)$$

Here Q_e , Q_- and Q_+ are the source terms as $Q_e = (\nu_{ion} - \nu_a) n_e + \nu_d n_- - \beta_{e+} n_e n_+ - n_e / \tau$, $Q_- = \nu_a n_e - \nu_d n_- - \beta_{ii} n_- n_+$. ν_{ion} , ν_a , ν_d are, respectively, the ionization, attachment and detachment frequencies. β_{e+} and β_{ii} are the reaction coefficients for the electron-ion and ion-ion recombination. μ_e , μ_- and μ_+ are the mobilities for electrons and ions. D_e is the electron diffusion coefficient, and τ is the characteristic time for convective removal of charged particles and heat from the discharge. As quasi-neutrality of the plasma is assumed, i.e. $n_+ = n_- + n_e$, Eqn. 4 is equivalent to

$$O \cdot [(\mu_e n_e + \mu_- n_- + \mu_+ n_+) E + D_e O n_e] = 0 \quad (5)$$

from which the radial-dependent electric field E_r can be determined. The characteristic electric field E_z between the two electrodes can be found from the current-voltage characteristic as

$$E_z = I / \int_0^{r_{max}} 2\pi r \sigma dr \quad (6)$$

Here the discharge current, I , is determined by the external electric circuit. σ is the conductivity of the quasi-neutral plasma and can be written as $\sigma = e(\mu_e n_e + \mu_- n_- + \mu_+ n_+)$.

As the pressure is equalized quickly, we can assume that the gas is heated under isobaric conditions. By applying the ideal-gas law, the gas density, ρ , and temperature, T , are related as $\rho \propto T^{-1}$. The governing equation for the gas translational temperature is

$$\rho c_p \frac{\partial T}{\partial t} - O \cdot (\lambda O T) = Q_t \quad (7)$$

where $Q_t = \eta_t j E + (E_v \frac{\partial}{\partial t} \text{[redacted]} + Q_c)$, c_p is the specific heat of the mixture at the constant pressure; λ is the heat conductivity; η_t is the fraction of Joule heating

responsible for the direct heating of the gas. Q_c accounts for the heat release or absorption during the plasma assisted fuel pyrolysis and oxidation process. Another two terms from vibrational to translational (V-T) energy relaxation are also included, which are related with the fact that a significant fraction of the deposited power in molecular discharges is pumped to the vibrational degrees of freedom and then released to translational degrees of freedom. The balance equation for vibrational energy, E_v , is

$$\frac{\partial}{\partial t} E_v - O \cdot (DOE_v) = Q_v \quad (8)$$

where $Q_v = \frac{1}{2} \cdot D \cdot \nabla^2 E_v + E_v \cdot \frac{1}{\tau} + \eta \cdot \omega \Pi$. D is the diffusion coefficient, E_v is the equilibrium value of E_v ; τ is the V-T relaxation time; η is the fraction of Joule heat responsible for the vibrational excitation. $\omega \Pi$ accounts for the flow of vibrational quanta in the vibrational energy domain due to V-V energy relaxation. Combustion species are also updated by calling the CHEMKIN II package [15]. Eqn. (2-8) form the simplified governing equations for the current plasma combustion system.

3. Results and Discussions

The dynamics of the above plasma-combustion system is highly dependent of its source terms, which contain both plasma kinetics and combustion kinetics. Those reaction kinetics determined by the mixture composition, electron and gas temperatures create the coupling between plasma thermal instability and plasma chemical instability (shown in Fig. 2)

For plasma kinetics, we consider electron-impact ionization, electron attachment and detachment, electron-ion and ion-ion recombination, and V-V and V-T energy relaxation. Electron attachment, detachment and the presence of negative ions are highly associated with electronegative gases in the mixture. Since in all the cases presented in this work the value of electron temperature does not exceed 0.8-1.5 eV for the entire range of E/N , we consider only the electron attachment in the three-body collisions as $e^- + M \rightarrow e^- + M$ (M is a third-body). Besides, the vibrational-translational (V-T) energy relaxation time scales are different among species. In the $H_2-O_2-N_2$ mixture, we assume most vibrational energy is stored in the nitrogen molecules in view of rapid V-T relaxation of oxygen molecules [14]. The set of parameters are obtained via various literature [13, 14, 16, 17]. For combustion kinetics, we use the sub-mechanism for $H_2-O_2-N_2$ kinetics adapted from the well-validated HP Mech at Princeton [18, 19, 20], which includes 22 elementary reactions and 9 species. (See Supplementary Material for more details about plasma and combustion kinetics).

+ M (M is a third-body). Besides, the vibrational-translational (V-T) energy relaxation time scales are different among species. In the $H_2-O_2-N_2$ mixture, we assume most vibrational energy is stored in the nitrogen molecules in view of rapid V-T relaxation of oxygen molecules [14]. The set of parameters are obtained via various literature [13, 14, 16, 17]. For combustion kinetics, we use the sub-mechanism for $H_2-O_2-N_2$ kinetics adapted from the well-validated HP Mech at Princeton [18, 19, 20], which includes 22 elementary reactions and 9 species. (See Supplementary Material for more details about plasma and combustion kinetics).

3.1. Effect of Fuel Pyrolysis

We first investigate the effect of plasma enhanced fuel pyrolysis on the onset of plasma instability by comparing the current-voltage characteristics in $\text{N}_2\text{-O}_2$ and $\text{N}_2\text{-H}_2$ mixtures shown in Fig. 3. The top (blue) traces correspond to the uniform state of the volumetric plasma discharge while the bottom (red) symbols correspond to the contracted states after plasma instability. The vertical dashed lines represent the onset or transition limits between volumetric and contracted plasma states. Clearly, one can see a large shift of the critical current of the onset of plasma instability. The $\text{N}_2\text{-H}_2$ mixture system is more stable than the $\text{N}_2\text{-O}_2$ system. The higher ionization potential (H_2 : 15.40 eV, O_2 : 12.06 eV [21]) of H_2 and endothermic H_2 pyrolysis reactions make the $\text{N}_2\text{-H}_2$ system more

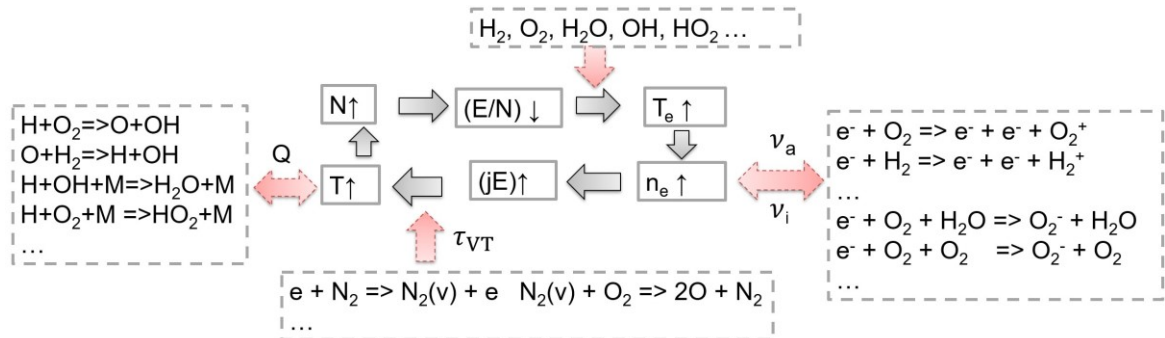


Figure 2: The schematic of the coupled plasma thermal-chemical mechanism in the plasma assisted ignition. Black arrows (solid) refer to the original feedback in the plasma thermal instability. Red arrows (dotted) are some new couplings from the plasma chemical instability. Q is the heat absorption or heat release from combustion. τ_{VT} refers to the timescale of the V-T relaxation process. ν_i and ν_a refer to plasma kinetic processes including ionization or attachment of combustion species.

difficult to produce electron and increase the temperature. The steady-state distribution of reduced electron field for two mixtures are also shown in Fig. 4. The presence of H_2 lowers the peak reduced electric field, thus reduces electron number density. As a result, the plasma combustion chemistry inhibits the plasma instability. Therefore, the increased fuel ionization potential and the endothermic plasma enhanced fuel pyrolysis process is one mechanism of the plasma chemical instability.

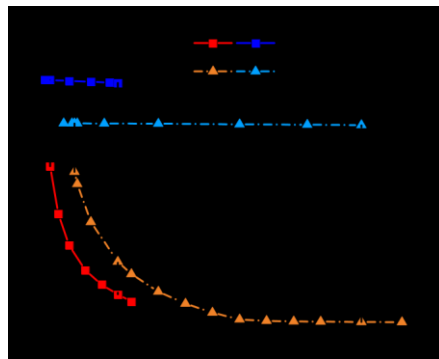


Figure 3: Comparison of current-voltage characteristics with different compositions. $p = 50$ Torr, Convective time scale $\tau = 10^{-3}$ s. (Squares correspond to N_2/O_2 mixtures, triangles correspond to N_2/H_2 mixtures.)

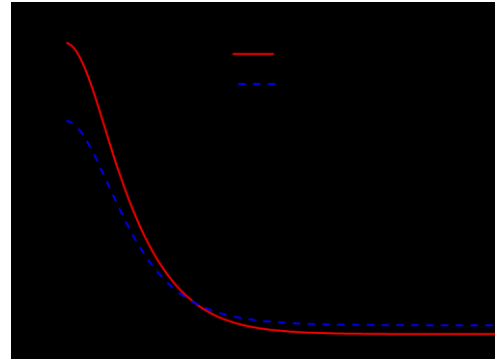


Figure 4: Comparison of steady-state distribution of reduced electric field (Td) for different mixture compositions. $p = 50$ Torr, Convective time scale $\tau = 5 \times 10^{-3}$ s. $I = 35$ mA.

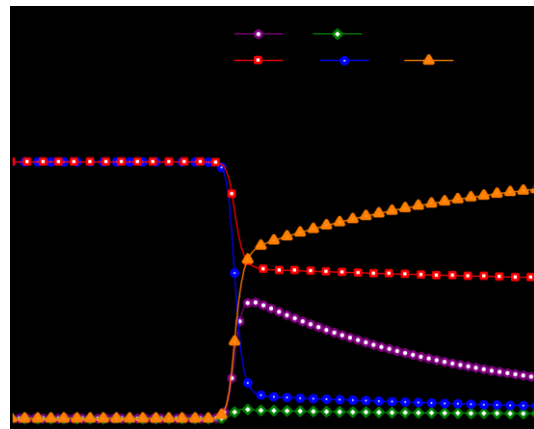


Figure 5: Time histories of species and temperature at the center of the computational domain at 0.02 s - 0.03 s. The onset of plasma thermal-chemical instability occurs at 0.023 s. $p = 50$ Torr. Convective time scale $\tau = 10^{-3}$ s. $I = 30$ mA.

3.2. Effect of Exothermic Fuel Oxidation

We now consider a fuel-lean $\text{H}_2\text{-N}_2\text{-O}_2$ mixture system to examine the effect of fuel oxidation kinetics on the plasma instability.

Firstly, we examined the time histories of temperature and species at the center of the computational domain ($r=0$). The initial mixture composition ratio was $N_2-H_2-O_2=80:10:10$ at room temperature. From Fig. 5, the thermal-chemical instability happened with a sharp energy release and a rapid temperature increase from Joule heating and V-T energy relaxation within $O(10^{-3} \text{ s})$. Then, heat generated from plasma thermal instability was consumed to decompose fuel molecules and initiate combustion chemical kinetics. Combustion intermediates including OH and H were formed and reacted promptly within $O(10^{-2} \text{ s})$. In a longer time scale as $O(10^{-1} \text{ s})$, the plasma enhanced combustion heat release increased the temperature shown in Fig. 6. The concentration of intermediate species decreased and the product of H_2O gradually reached its chemical-equilibrium state. Several key reactions were involved in the plasma assisted low temperature fuel oxidation process as $H + O_2 \rightarrow O + OH$ and $H + OH + M \rightarrow H_2O + M$. After that, the chemical effect on plasma instability was minimal as the mixture was no longer reactive.

To further demonstrate the chemical effect on the plasma instability in a quasi-steady state system, the fuel-lean mixtures into the domain were continuously flowed into the system. As shown in Fig. 7, the mole fractions of combustion products converged to their steady state values quickly. and play a lasting role in the development of plasma chemical instability (shown in Fig. 7). The hysteresis of current-voltage characteristics is shown in Fig. 8. With plasma enhanced exothermic fuel oxidation, the critical current for the transition from homogeneous plasma state to contracted plasma state is decreased and the resulting hysteresis region is more narrowed, indicating that the plasma assisted low temperature fuel oxidation process at the high current makes the system more unstable. This is the second mechanism of plasma chemical instability.

Clearly plasma assisted combustion heat release can significantly modify the stability boundary of plasma by increasing temperature and increase the reduced field. Moreover, it will also modify the thermal diffusion process and stabilize the plasma. Furthermore, the plasma assisted fuel oxidation process changes the compositions and therefore the mixture plasma properties. We further evaluate the individual contribution from plasma assisted combustion heat release and the change of mixture properties by combustion (shown in Table. 1). At high current, i.e. high temperature (over 1,000 K), without considering the combustion heat release, the temperature difference is considerable. The peak vibrational temperature in the fuel-lean mixture is also higher, indicating a higher degree of plasma non-equilibrium. However, at low current, i.e. low temperature (lower than 800 K), combustion heat release from the H_2-O_2 mixture is negligible. Nevertheless, the peak temperature in the oxidation case is still higher than the non-oxidation case, indicating that the change of mixture properties due to fuel oxidation is the dominant mechanism for plasma chemical instability at low temperature. More investigations of how fuel oxidation would change the mixture plasma property is required.

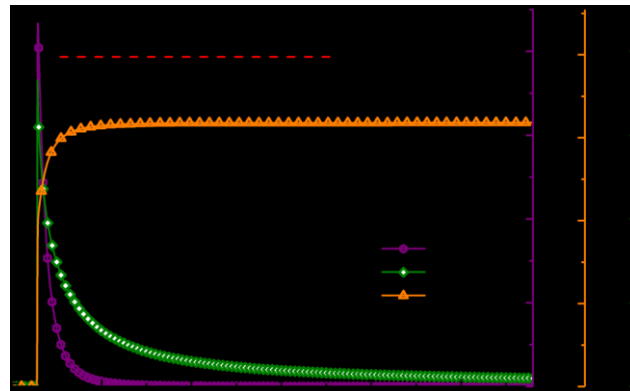


Figure 6: Time histories of species and temperature at the center of the computational domain at 0.01 s - 0.3 s. After the onset of plasma instability, the temperature reaches its local minimum of 1112 K at $t=0.37$ s. Then, the temperature gradually increases. The red dotted line indicates the constant temperature of $T = 1112$ K. $p = 50$ Torr. Convective time scale $\tau = 10^{-3}$ s. $I = 30$ mA.

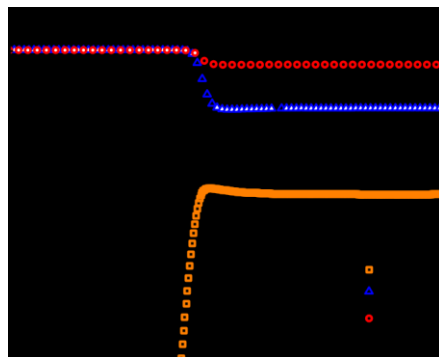


Figure 7: Time histories of species and temperature at the center of the computational domain at $t = 0.018$ s - 0.025 s. The initial mixture composition ratio is $N_2-H_2-O_2 = 40 : 30 : 30$. The fuel-lean H_2-O_2 mixture flows continuously into the

system with a speed of 1.17 mol/s. Species and temperature reach steady states after $t=0.02$ s. $p = 50$ Torr. Convective time scale $\tau = 10^{-3}$ s. $I = 30$ mA.

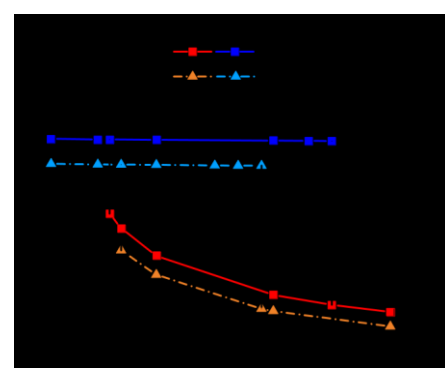


Figure 8: Comparison of current-voltage characteristics with and without fuel oxidation. (Squares correspond to non-reacting $\text{N}_2\text{-O}_2$ mixtures, triangles correspond to $\text{N}_2\text{-O}_2\text{-H}_2$ mixtures. Initial mixture composition ratio is $\text{N}_2 : \text{O}_2 : \text{H}_2 = 80 : 6.7 : 13.3$).

13.3. The $\text{N}_2\text{-O}_2\text{-H}_2$ mixture flows continuously into the system with speed of 1.17×10^{-7} mol/s. $p = 50$ Torr.

Convective time scale $\tau = 10^{-3}$ s. $I = 30$ mA.

Table 1: Peak Vibrational and Translational Temperature in 1D domain with or without fuel oxidation

Mixture Compositions	T, K	I=10 mA	I= 20 mA	I= 29 mA
$\text{N}_2\text{-O}_2 = 80 : 20$	$T_{v,\text{max}}$	4365	5209	5688
	T_{max}	623	850	997
$\text{N}_2\text{-O}_2\text{-H}_2 = 80 : 6.7 : 13.3$	$T_{v,\text{max}}$	4428	5275	5765
	T_{max}	632	864	1018
$\text{N}_2\text{-O}_2\text{-H}_2 = 80 : 6.7 : 13.3$ (neglect Q from combustion)	$T_{v,\text{max}}$	4428	5256	5741
	T_{max}	632	854	1006

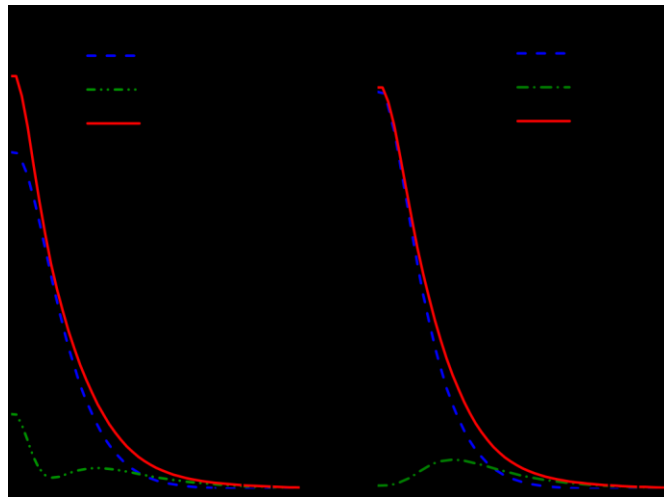


Figure 9: Comparison of the steady-state distributions of charge particles for $k_a \sim 10^{-31} \text{ cm}^6 \text{ s}^{-1}$ and $k_a \sim 10^{-32} \text{ cm}^6 \text{ s}^{-1}$. $p = 50 \text{ Torr}$. Convective time scale $\tau = 10^{-3} \text{ s}$. $I = 30 \text{ mA}$.

3.3. Effect of Electron Attachment

Electron attachment is another key kinetic process in plasma chemistry instability. Combustible mixtures typically have higher concentrations of water and oxygen, leading to a higher attachment rate by several orders of magnitude compared with air or other diluents (shown in Table. 2).

By artificially perturbing the overall attachment rate, we observed different steady-state distributions of charged particles (shown in Fig. 9). With a higher attachment rate, more electrons were attached to molecules, yielding a higher population of negative ions. When the plasma chemical instability was triggered, the increase of negative ions and decrease of electron number density decreased the overall charge particle mobility and thus stabilized the system. Therefore, high electron attachment rate to oxygen and water will suppress the electron production and plasma chemical instability. With the increase of oxygen concentration in a combustible mixture, there is a competition between plasma assisted heat release and electron attachment to oxygen in PCI. Higher oxygen concentrations lead to strong electron attachment, which stabilizes PCI. Meanwhile, higher oxygen content also enhances the oxidation process, which would promote radical production and heat release processes, resulting in destabilization of the system.

Table 2: Reaction rate coefficients of electron attachment to oxygen molecules at room temperature and different third body partners

Three body attachment to oxygen	Rate coefficient [22]
e + O ₂	2×10^{-31} cm ⁶ /s
e + O ₃	1.6×10^{-31} cm ⁶ /s
e + O ₂ ⁺	2.5×10^{-30} cm ⁶ /s
e + O ₃ ⁺	1.4×10^{-29} cm ⁶ /s

4. Conclusion

A new concept of plasma chemical instability (PCI) caused by plasma combustion chemistry is presented and analyzed in plasma assisted combustion. The results show that the plasma chemical instability significantly affects the critical plasma current for transition between the volumetric discharge and the contracted discharge defined by the plasma thermal instability. The plasma chemical instability can couple with the plasma thermal instability via the endothermic and exothermic plasma assisted combustion reactions by changing the local temperature. Moreover, the electron attachment to oxygen and combustion products as well as the change of plasma properties in combustion process also contribute to the plasma chemical instability without plasma assisted combustion heat release. Specifically, the results reveal that the endothermic electron-impact fuel dissociation and excitation reactions and electron attachment processes will increase the plasma stability. Moreover, plasma assisted low temperature combustion heat release will promote the plasma instability. Furthermore, energy relaxation via vibrational modes and V-T energy transfer also affect the onset of plasma instability. Future modeling with detailed chemical kinetics is necessary for quantitative studies of plasma chemical instability with strong non-equilibrium of plasma energy distributions at high electric field strength.

Acknowledgments

This work was supported by NSF and DOE Grant on plasma instability and plasma chemistry. We thank Dr Shuqun Wu for helpful discussions in stability analysis of PCI. We also thank Mr Xingqian Mao, Timothy Chen, and Aric Rousso for the insightful discussions of plasma-assisted combustion kinetics.

References

- [1] D. Dunn-Rankin. *Lean combustion: technology and control*. Academic Press, 2011.
- [2] V. Ganesan. *Internal combustion engines*. McGraw Hill Education (India) Pvt Ltd, 2015.
- [3] V. McDonell. Lean combustion in gas turbines. In *Lean Combustion*, pages 147–201. Elsevier, 2016.
- [4] Z. Chen and Y. Ju. Theoretical analysis of the evolution from ignition kernel to flame ball and planar flame. *Combustion Theory and Modelling*, 11(3):427–453, 2007.
- [5] S. H. Won, S. Dooley, P. Veloo, J. S. Santner, Y. Ju, and F. L. Dryer. Characterization of global combustion properties with simple fuel property measurements for alternative jet fuels. In *50th AIAA/ASME/SAE/ASEE Joint Propulsion Conference*, page 3469, 2014.
- [6] S. M. Starikovskaia. Plasma assisted ignition and combustion. *Journal of Physics D: Applied Physics*, 39(16):R265, 2006.
- [7] S. M. Starikovskaia. Plasma-assisted ignition and combustion: nanosecond discharges and development of kinetic mechanisms. *Journal of Physics D: Applied Physics*, 47(35):353001, 2014.
- [8] Y. Ju and W. Sun. Plasma assisted combustion: Dynamics and chemistry. *Progress in Energy and Combustion Science*, 48:21–83, 2015.
- [9] E. M. Bazelyan, Y. P. Raizer, and N. L. Aleksandrov. The effect of reduced air density on streamer-to-leader transition and on properties of long positive leader. *Journal of Physics D: Applied Physics*, 40(14):4133, 2007.
- [10] E. P. Velikhov, V. S. Golubev, and S. V. Pashkin. Glow discharge in a gas flow. *Soviet Physics Uspekhi*, 25(5):340, 1982.
- [11] Y. P. Raizer. *Gas discharge physics*. 1991.
- [12] A. V. Eletskii and B. M. Smirnov. Nonuniform gas discharge plasma. *Physics Uspekhi*, 39(11):1137, 1996.
- [13] M. N. Shneider, M. S. Mokrov, and G. M. Milikh. Dynamic contraction of the positive column of a self-sustained glow discharge in molecular gas. *Physics of Plasmas*, 19(3):033512, 2012.

REFERENCES

- [14] M. N. Shneider, M. S. Mokrov, and G. M. Milikh. Dynamic contraction of the positive column of a self-sustained glow discharge in air flow. *Physics of Plasmas*, 21(3):032122, 2014.

- [15] R. J. Kee, F. M. Rupley, and J. A. Miller. Chemkin-ii: A fortran chemical kinetics package for the analysis of gas-phase chemical kinetics. Technical report, Sandia National Labs., Livermore, CA (USA), 1989.
- [16] A. V. Phelps. Electron transport data, 1998.
- [17] N. L. Aleksandrov. Three-body electron attachment to a molecule. *Soviet Physics Uspekhi*, 31(2):101, 1988.
- [18] M. P. Burke, M. Chaos, Y. Ju, F. L. Dryer, and S. J. Klippenstein. Comprehensive h₂/o₂ kinetic model for high-pressure combustion. *International Journal of Chemical Kinetics*, 44(7):444–474, 2012.
- [19] J. Santner, F. L. Dryer, and Y. Ju. The effects of water dilution on hydrogen, syngas, and ethylene flames at elevated pressure. *Proceedings of the Combustion Institute*, 34(1):719–726, 2013.
- [20] S. Yang, X. Yang, F. Wu, Y. Ju, and C. K. Law. Laminar flame speeds and kinetic modeling of h₂/o₂/diluent mixtures at sub-atmospheric and elevated pressures. *Proceedings of the Combustion Institute*, 36(1):491–498, 2017.
- [21] K. Watanabe. Ionization potentials of some molecules. *The Journal of Chemical Physics*, 26(3):542–547, 1957.
- [22] A. Fridman. *Plasma chemistry*. Cambridge university press, 2008.